Effective Optimization of the Control System for the Cement Raw Meal Mixing Process: I. PID Tuning Based on Loop Shaping

DIMITRIS TSAMATSOULIS
Halyps Building Materials S.A., Italcementi Group
17th Klm Nat. Rd. Athens – Korinth
GREECE
d.tsamatsoulis@halyps.gr http://www.halyps.gr

Abstract: - The objective of the present study is to use a reliable model of the raw meal mixing process dynamics in raw meal production installations, in order to tune effectively PID controllers, thus regulating the product's quality. The system is described by a TITO process. The M - Constrained Integral Gain Optimization (MIGO) loop shaping method is utilized to adjust the controller parameters. Long term actual industrial data are used for this purpose while the controller robustness is also investigated. Taking into account the maximum sensitivity constraint and the model uncertainty the controller is parameterized and implemented to industrial raw meal production units by replacing previous controllers or manual regulation. The results indicate remarkable enhancement of the raw meal homogeneity fed to the kiln. Therefore the tuning methodology applied provides effective PID controllers, able to attenuate the disturbances affecting the raw meal quality.

Key-Words: - Dynamics**,** Raw meal, Quality, Mill, Model, Uncertainty, PID, Robustness, Sensitivity

1 Introduction

The main factor that primarily affects the cement quality is the variability of the clinker activity [1], depending on the conditions of the clinker formation and the raw meal composition.

In Figure 1 a typical flow chart of raw meal production is shown.

The fine exit stream of the separator is the main part of the final product. The coarse separator return is directed to the mill, where it is ground and from there, via the recycle elevator, it feeds the separator. The materials in the mill and classifier are dried and de-dusted by hot gas flow.
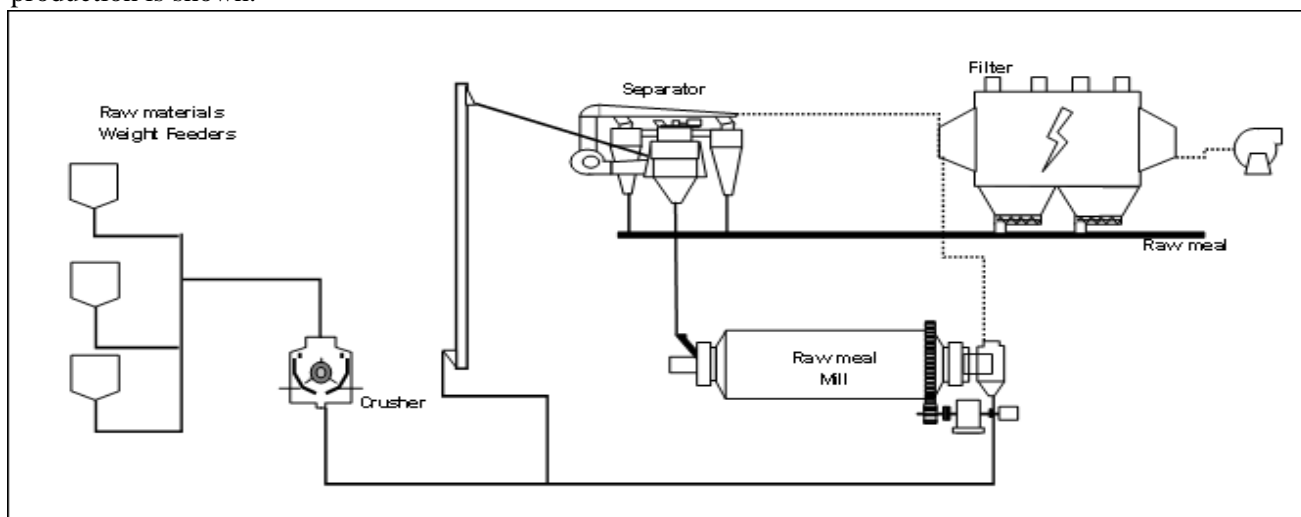

Figure 1. Flow chart of raw meal production

In the closed circuit process demonstrated, the raw materials' feeding is performed via three weight feeders, firstly feeding a crusher. The crusher outlet goes to the recycle elevator and from there it advances to a dynamic separator, the speed and gas flow of which controls the product fineness. The

This is a standard flow sheet encountered to the most of the raw meal dry grinding processes performed in ball mills.

The raw mix composition stability not only has an impact on the clinker composition but it also affects the kiln thermal consumption and bricks lining and the conditions of the clinker formation. So, keeping

the raw meal quality in the kiln feed as much stable as possible is of high importance.

The variation of this parameter is related to the homogeneity of the raw materials in the raw mill (RM) inlet, to the mixing efficiency of the homogenizing silo and to the regulation effectiveness as well. Due to its complexity and significance, different automated systems are available for sampling and analyzing the raw mix as well as for the adjustment of the mill weight feeders according to the raw meal chemical modules in the RM outlet [2]. The regulation is mainly obtained via PID and adaptive controllers. Ozsoy et al. [3] developed three different linear multivariable stochastic models to describe the dynamics of a raw blending system. Kizilaslan et al. [4] performed a comparative study on modeling of raw meal blending process using conventional and intelligent techniques. Kural et al. [5] built on stochastic multivariable dynamic models and designed model predictive controllers to calculate the optimal feed ratios of the raw materials despite disturbances. As the authors clearly declare, the disturbances coming from the variations in the chemical compositions of the raw materials from long-term average compositions cause the changes of the system's parameters. Tsamatsoulis [6] built a reliable model of the dynamics among the chemical modules in the outlet of a raw meal grinding system and the proportion of the raw materials. The model developed can feed with inputs advanced automatic control implementations, in order a robust controller to be achieved, able to attenuate the disturbances affecting the raw meal quality. As Jing et al. state [7], the modeling of the uncertainties or the handling of the deterministic complexity is typical problems, frequently encountered in the field of systems and control engineering. For this and other reasons mentioned in [8], special attention is paid to the problems of the synthesis of complex systems' dynamical models, to the construction of efficient control models, and to the development of simulation. As a result, to design a robust controller, satisfying a given sensitivity constraint [9, 10] an efficient modeling of the process is obligatory.

Several adaptive controllers of varying degrees of complexity have been also developed [11, 12]. Banyasz at al. [12] presented the control algorithm in a technology-independent manner. Duan et al. [13] presented a case study on the practical implementation of a hybrid expert system for a raw materials blending process. Additionally to the previous attempts and realizations and due to the complexity and high degree of uncertainty fuzzy controllers are also developed [14, 15]. However, it has been mentioned by Astrom et al. [16] that, in the industrial process control, more than 95% of the control loops are of PID type. Moreover, only a small portion of them operates properly as Ender [17] points out. Frequently, also, the controller parameters are tuned with trial and error [18], because of the lack of a model or of a high model uncertainty. Tsamatsoulis [19] tuned a classical PID controller among chemical modules in the RM output and raw materials proportion in the mill feed, using the minimum standard deviation of these modules in the kiln feed as an optimization criterion. He concluded that the application of the stability criteria is necessary. He, also, proved that the variance of the kiln feed composition not only depends on the raw materials variations and the mixing capacity of the silos, but it is also strongly related with the effectiveness of the regulating action. As it was clearly stated by Astrom [20], model uncertainty and robustness have been a central theme in the development of the field of automatic control. A widely applied methodology to derive robust and efficient controllers is the loop shaping technique [21, 22, 23], the so-called H∞ theory [25, 26, 27, 28, 29, 30]. An extremely efficient loop shaping technique to tune PID controllers is called MIGO (M- constrained integral gain optimization) [31, 32, 33, 34]. The design approach is to maximize integral gain subject to a constraint on the maximum sensitivity.

The aim of the present study is to tune a classical PID controller, regulating the LSF and SM modules in the raw mill (RM) outlet using the feeders' dosages as control variables. The dynamical model developed and described in [6] is utilized. All the main components of the process are expressed with the respective transfer functions. The model mean parameters and their uncertainty are evaluated using actual process data of Halyps' cement plant. The MIGO method is implemented using as robustness criterion the maximum sensitivity M_s. The interaction of the two loops under the actual operating conditions and raw materials is also investigated. Using the error propagation technique, the uncertainty of the closed loop properties is expressed as a function of the model parameters' variance and the results are being analyzed. The implementation of the mentioned tuning technique to the PID regulating the Halyps raw meal is also demonstrated and compared with previous data of automatic operation. Due to the general characteristics of the methodology and its extremely positive results of industrial application, this type of tuning is already applied to a significant number of other raw mills.

2 Process Model

2.1 Proportioning Moduli Definition

The proportioning moduli are used to indicate the quality of the raw materials and raw meal and the clinker activity too. For the main oxides, the following abbreviations are commonly used in the cement industry: $C=CaO$, $S=SiO_2$, $A=Al_2O_3$, $F=Fe_2O_3$. The main moduli characterizing the raw meal and the corresponding clinker are as follow [1]:

$$Lime\ Saturation\ Factor$$
$$LSF = \frac{100 \cdot C}{2.8 \cdot S + 1.18 \cdot A + 0.65 \cdot F} \quad (1)$$

$$Silica\ Modulus \quad SM = \frac{S}{A + F} \quad (2)$$

$$Alumina\ Modulus \quad AM = \frac{A}{F} \quad (3)$$

The regulation of some or all of the indicators (1) to (3) contributes drastically to the achievement of a stable clinker quality.

2.2 Block Diagram

The block diagram is presented and analyzed in [6] and repeated here for elucidation reasons. The block diagram is illustrated in Figure 2, where the controller block also appears.
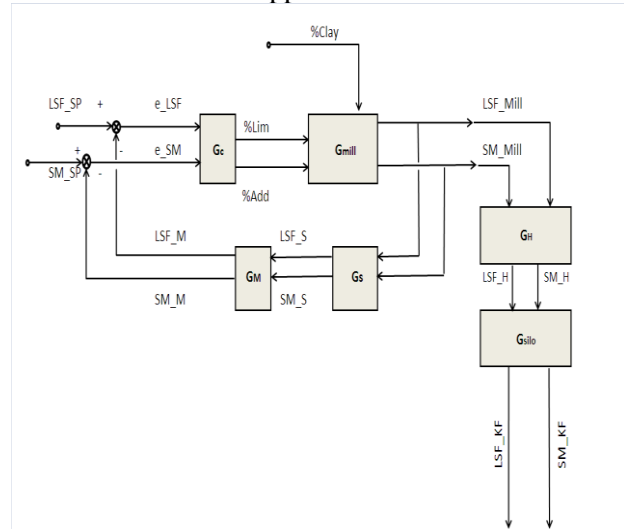

Figure 2. Flow chart of the grinding and blending process.

Each block represents one or more transfer function: G_c symbolizes the transfer function of the controller. With G_{mill}, the RM transfer function is indicated, composed from three separate functions. During the sampling period, a sampling device accumulates an average sample. The integrating action of the sampler during the time interval between two consecutive samples is denoted by the function G_s. The delay caused by the sample analysis is shown by the function G_M.

The homogenization is performed in overflow homogenizing silo with transfer function G_H. Then the raw meal before to enter to the kiln, is stocked to a stock silo with transfer function G_{silo}.

%Lim, %Add, %Clay = the percentages of the limestone, additive and clay in the three weight feeders. LSF_{Mill}, SM_{Mill} = the spot values of LSF and SM in the RM outlet, while LSF_S, SM_S, LSF_M, SM_M = the modules of the average sample and the measured one. Finally LSF_H, SM_H, LSF_{KF}, SM_{KF} = the corresponding modules in the homo silo outlet and in the kiln feed. The LSF and SM set points are indicated by LSF_{SP} and SM_{SP} respectively, while e_LSF and e_SM stand for the error between set point and respective measured module.
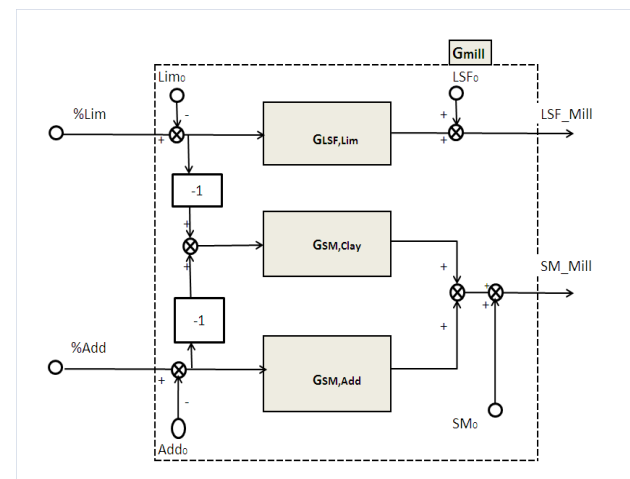

Figure 3. Transfer functions of the RM block.

The transfer function of the raw meal mixing in the RM is analyzed in more detail in Figure 3.The functions between the modules and the respecting percentages of the raw materials are indicated by $G_{LSF,Lim}$, $G_{SM,Clay}$, $G_{SM,Add}$. The constant denoted by the subscript "0" will be explained in the next section. This configuration includes some simplifications and assumptions which are proved as valid in connection with the current raw materials analysis:

- There is not effect of the additive on the LSF as its percentage is very low, less than 3%.
- The materials humidity is neglected, to simplify the calculations.
- As to the clay, the function %Clay=100-%Lim-%Add is taken into account.

2.3 Process Transfer Functions

For the existing RM circuit, the objective of the analysis is to model the transfer function between the raw meal modules in the RM outlet and the proportions of the raw materials in the feeders. To model also the transfer function of the homo and stock silo in order to be possible to optimize the controllers using process simulations. Consequently for the functions G_{mill}, G_s, G_M, G_H, G_{Silo} analytical equations in the Laplace domain are needed. The G_M represents a pure delay, therefore is given by equation (4):

$$G_M = e^{-tM \cdot s} \tag{4}$$

The delay t_M is composed by the time intervals of sample transferring, preparation, analysis and computation of the new settings of the three feeders and finally transfers of those ones to the weight scales. For the given circuit the average $t_M = 25$ min $= 0.42$ h. By the application of the mean value theorem and the respective Laplace transform, the function G_s is calculated by the formula (5):

$$G_s = \frac{1}{T_s \cdot s} (1 - e^{-Ts \cdot s}) \tag{5}$$

The sampling period T_s is equal to 1 h. Based on the step response results of [19], performed in the same RM a second order with time delay (SOTD) model is chosen for each of the functions $G_{LSF,Lim}$, $G_{SM,Clay}$, $G_{SM,Add}$ described by the equation (6):

$$G_x = \frac{k_{g,x}}{\left(1 + T_{0,x} \cdot s\right)^2} \cdot e^{-td,x \cdot s} \tag{6}$$

Where x = Lim, Clay or Add. The constant k_g, T_0, t_d symbolize the gain, the time constant and the time delay respectively. The values of these nine variables shall be estimated. As measured inputs and outputs of the process are considered the %Lim and %Add as well as LSF_M and SM_M. In the time domain the functions (6) are expressed by the equations (7) and (8):

$$LSF - LSF_0 = k_{g,Lim} \cdot (1 - \exp\left(-\frac{t - t_{d,Lim}}{T_{0,Lim}}\right) -$$
$$\frac{t - t_{d,Lim}}{T_{0,Lim}} \cdot \exp\left(-\frac{t - t_{d,Lim}}{T_{0,Lim}}\right)) \cdot (Lim - Lim_0) \tag{7}$$

The Lim_0 and LSF_0 parameters stand for the steady state values of the input and output variables.

The $Clay_0$, Add_0 and SM_0 parameters correspond to the steady state values. $Clay_0$ is not an independent variable but given from the difference 100- Lim_0-Add_0. The LSF and SM variables of the functions (7),(8) represent the RM outlet LSF and SM that also corresponds to the homo inlet $LSF_{H,In}$, $SM_{H,In}$.

$$SM - SM_0 = k_{g,Clay}$$
$$\cdot \left(\begin{array}{c} 1 - \exp\left(-\frac{t - t_{d,Clay}}{T_{0,Clay}}\right) \\ -\frac{t - t_{d,Clay}}{T_{0,Clay}} \cdot \exp\left(-\frac{t - t_{d,Clay}}{T_{0,Clay}}\right) \end{array} \right)$$
$$\cdot (Clay - Clay_0) + k_{g,Add}$$
$$\cdot \left(\begin{array}{c} 1 - \exp\left(-\frac{t - t_{d,Add}}{T_{0,Add}}\right) - \frac{t - t_{d,Add}}{T_{0,Add}} \\ \cdot \exp\left(-\frac{t - t_{d,Add}}{T_{0,Add}}\right) \end{array} \right)$$
$$\cdot (Add_0 - Add) \tag{8}$$

To avoid elevated degrees of freedom the following equalities are considered:

$$T_{0,Clay} = T_{0,Add} \quad t_{d,Clay} = t_{d,Add} \tag{9}$$

The homo and stock silo transfer functions are given by the first order equations (10) and (11) respectively:

$$G_H = \frac{y_H}{y_{H,In}} = \frac{1}{1 + T_H \cdot s} \tag{10}$$

$$G_{Silo} = \frac{y_{KF}}{y_H} = \frac{1}{1 + T_{Silo} \cdot s} \tag{11}$$

Where y_H=LSF_H or SM_H, $y_{H,In}$=$LSF_{H,In}$ or $SM_{H,In}$, y_{KF}=LSF_{KF} or SM_{KF}. T_H and T_{Silo} represent the homo and stock silo first order time constants.

2.4 Parameters Estimation Procedure

The procedure to estimate the mean parameters of the raw mill dynamics and their uncertainty as well is analytically described in [6]. To evaluate the RM model parameters, data of feeders' percentages and proportioning modules for the first seven months of 2010 are accessed. Afterwards using the specific software presented in [6]:

(i)   Continuous RM operation time intervals are found.

(ii)   For each set of M continuous data a subset of N=14 consecutive samples is taken using a moving window technique.

(iii) For each subset and using a non linear regression technique the optimum model parameters are computed as well as the regression coefficient, R.

(iv) A threshold of $R_{Min} \geq 0.7$ is chosen and the results are screened.

(v) The average and standard deviation of these results are determined.

(vi) The total number of subsets was 739. As to LSF dynamics a 53% of them presented $R \geq R_{Min}$. The corresponding value for the SM dynamics was 73%. The results are depicted in Table 1.

Table 1. Average and standard deviation of the model parameters

	Average	Standard Dev.
$K_{g,Lim}$	2.96	0.82
$T_{0,Lim}(h)$	0.19	0.15
$t_{d,Lim}(h)$	0.41	0.13
$K_{g,Clay}$	0.036	0.030
$K_{g,Add}$	0.437	0.291
$T_{0,Clay}(h)$	0.33	0.18
$t_{d,Clay}(h)$	0.33	0.18

To have a verification of the estimated gains using the seven months operating data, the average analysis of the raw materials of the same year are also utilized. By implementing mix design software to compute the raw meal composition for given feeders' composition, the static gains between inputs and outputs are determined, e.g. the increase or decrease of the modules is found for 1% increase of each compound. The gain between LSF and %additive is also found. The results are shown in table 2.

Table 2. Static gain between feeders' dosage and chemical modules

$K_{g,Lim}$	2.64
$K_{g,Clay}$	0.01
$K_{g,Add}$	0.388
$K_{LSF,Add}$	0.05

The procedure of the feeders' changes is the following: When the limestone or the additive feeders are increasing by 1%, then the clay feeder is decreasing by 1%. An increase of the additive by 1% results in a decrease of SM by $K_{g,Add}$=0.354 and of LSF by $K_{LSF,,Add}$=0.05. For the two other cases, an increase of the feeder results in an increase of the module. The combination of the slight changes of the additive with the small value of $K_{LSF,Add}$ in comparison with $K_{g,Lim}$ causes a

negligible effect of the additive changes to LSF value. Therefore the assumption made is section 2.2 is verified. All the static gains calculated from the mix design balances are found within the range of the gains shown in Table 2 taking into account their mean values and standard deviations.

The estimation of the homo and stock silos time constants cannot be achieved via the inlet and outlet LSF or SM. The reason is that these two modules are already regulated well enough using a PID controller tuned according to the method presented in [6] and any significant dynamics is not possible to be detected for a long period. For this reason the AM is chosen in the homo inlet and stock silo outlet and one full year data are accessed via the plant data base. The mill outlet and kiln feed flow rates are also considered. As the homo silo operates with overflow, it is always considered to be full. As to the stock silo, the empty meters during the operation are also taken into account. The processing of one full year data provided the following results:

$$T_H = 3.0 \pm 0.6 \, h$$

$$T_{Silo} = 16.3 \cdot H_E^{-0.6} \pm 1.3 \, h \qquad (12)$$

Where H_E= the empty meters of the stock silo. To notice that each meter of the stock contains 330 tons of raw meal.

2.5 Loops' Interaction

The process described constitutes a two inputs two outputs system (TITO). Therefore a search shall be made for probable interactions between the loops to be controlled. The investigation is based to Bristol Relative Gain Array – RGA- [35] having the ability to detect interactions for low frequency signals. In spite of the low gain the transfer function from %additive to LSF is also considered. The following variables are defined:

$$y_1 = LSF(s) - LSF_0 \, , \quad y_2 = SM(s) - SM_0 \qquad (13)$$
$$u_1 = Lim(s) - Lim_0 \, , \quad u_2 = Add(s) - Add_0 \qquad (14)$$

The TITO system is described by the following equations:

$$y_1 = G_{LSF,Lim} \cdot u_1 - G_{LSF,Add} \cdot u_2 \qquad (15)$$

$$y_2 = G_{SM,Clay} \cdot (-u_1 - u_2) - G_{SM,Add} \cdot u_2 \Rightarrow$$

$$y_2 = -G_{SM,Clay} \cdot u_1 - (G_{SM,Clay} + G_{SM,Add}) \cdot u_2 \qquad (16)$$

The RGA is defined from the formulae:

$$RGA = \begin{pmatrix} \lambda & 1-\lambda \\ 1-\lambda & \lambda \end{pmatrix} \qquad (17)$$

$$\lambda = \frac{p_{11}(0)p_{22}(0)}{p_{11}(0)p_{22}(0) - p_{12}(0)p_{21}(0)} \qquad (18)$$

Where:

$$p_{11} = G_{LSF,Lim}, \ p_{12} = -G_{LSF,Add}$$
$$p_{21} = -G_{SM,Clay}, p_{22} = -(G_{SM,Clay} + G_{SM,Add}) \qquad (19)$$

Therefore the parameter λ is computed from formula (20):

$$\lambda = \frac{-K_{g,Lim} \cdot (K_{g,Clay} + K_{g,Add})}{-K_{g,Lim} \cdot (K_{g,Clay} + K_{g,Add}) - K_{LSF,Add} \cdot K_{g,Clay}} \qquad (20)$$

By substituting the gains with the values of table 2, a $\lambda=0.9987$ is computed. Subsequently for the low frequencies there is not interaction between the two loops. This conclusion has the following consequence. The controller regulating the loop between LSF and limestone can be tuned by using only the transfer function $G_{LSF,Lim}$. For the tuning also of the controller regulating the SM by acting on additive feeder, the function $G_{SM,Clay}+G_{SM,Add}$ shall be used. The two terms of this transfer function have the same time constant and delay time. So the gain is equal to the sum of the two gains. Because $K_{g,Clay}<<K_{g,Add}$, then $G_{SM,Clay}+G_{SM,Add}\approx G_{SM,Add}$. So for the tuning of the SM controller at low frequencies, only the transfer function from %additive to SM shall be considered.

3 PID Controller Design

The LSF and SM controllers are implemented using the typical form according to Anstrom and Hagglund [16]. The transfer function is described by equation (21). The variables k_p, k_i, k_d represent the proportional, integral and differential gains of the controller:

$$\frac{u}{e} = k_p + \frac{k_i}{s} + k_d s \qquad (21)$$

Where e = LSF_{SP}-LSF_M or SM_{SP}-SM_M, u = %Lim or %Add, (k_p,k_i,k_d) = (k_{pLSF}, k_{iLSF}, k_{dLSF}) or (k_{pSM},k_{iSM},k_{dSM}). This equation is expressed by equation (22) in discrete time domain, where as time interval, the sampling period is considered.

$$u_n = u_{n-1} + k_p \cdot (e_n - e_{n-1}) + T_s \cdot k_i \cdot e_n$$
$$+k_d \cdot \frac{1}{T_s} \cdot (e_n + e_{n-2} - 2 \cdot e_{n-1}) \qquad (22)$$

As performance criterion the sensitivity function is defined, determined by the Laplace equation (22):

$$S = \frac{1}{1 + G_C G_p} \qquad (22)$$

The S function tells us how the closed loop properties are influenced by small variations in the process [20]. As robustness measure the maximum sensitivity represented by the equation (23) is utilized:

$$M_s = Max(|S(i\omega)|) \qquad (23)$$

As it can be observed in Figure 4, the variable $1/M_s$ can be understood as the shortest distance between the open loop G_cG_p Nyquist curve and the critical point (-1,0). In the same figure other properties also characterizing the system stability are depicted as well:

- the gain margin, g_m
- the gain crossover frequency, ω_{gc}
- the phase margin, φ_m
- the sensitivity crossover frequency, ω_{sc}
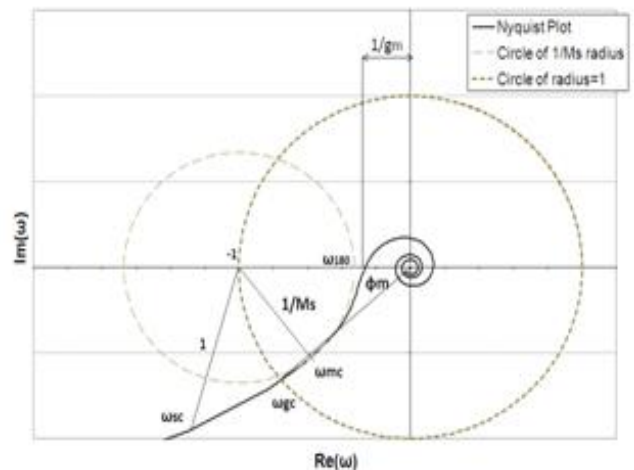- the maximum sensitivity crossover frequency, ω_{mc}.

Figure 4. Maximum sensitivity, phase margin and crossover frequencies

3.1 Implementation of the MIGO Method
One of the big advantages of the M- constrained Integral Gain Optimization design method is the guaranteed robustness. As shown in [16] the robustness conditions can be expressed in terms of

circles that are prohibited areas for the Nyquist plot of the open loop transfer function. The low frequency disturbances are attenuated from the integral gain of the PID controller. Therefore the maximization of the k_i part of the controller, by respecting the robustness conditions, contributes considerably to the rejection of the disturbances. The steps and the equations of the implementation of this technique in the specific application of the regulation of the raw meal quality are analyzed by demonstrating initially the system transfer function in the frequency domain:

From feeder X to module Y transfer function:

$$G_{Y,X}(i\omega) = \frac{K_g \cdot e^{-tdi\omega}}{(1 + iT_0\omega)^2} \qquad (24)$$

Where X = %Limestone, %Clay, %Additive and Y=LSF, SM.

Product of integrator and measurement transfer functions:

$$G_s(i\omega)G_M(i\omega) = \frac{1}{T_s \cdot i\omega}\left(1 - e^{-Ts \cdot i\omega}\right) \cdot e^{-tMi\omega} \qquad (25)$$

Process transfer function
$$G_P(i\omega) = G_{Y,X}(i\omega)G_s(i\omega)G_M(i\omega) \qquad (26)$$

The real and imaginary part of the process transfer function is given by the equations (27), (28).
$$ReG_p(\omega) = \frac{K_g}{T_s \cdot \omega \cdot (1 + \omega^2 T_0^2)^2} \cdot$$
$$\begin{pmatrix} -2\omega T_0 \cdot \left(\cos\left(\omega(t_M + t_d)\right) \cdot (1 - \cos\omega T_s) + \sin\left(\omega(t_M + t_d)\right)\sin\omega T_s\right) + \\ (1 - \omega^2 T_0^2) \cdot \left(\cos\left(\omega(t_M + t_d)\right)\sin\omega T_s + \sin\left(\omega(t_M + t_d)\right) \cdot (1 - \cos\omega T_s)\right) \end{pmatrix}$$

$$(27)$$

$$ImG_p(\omega) = \frac{K_g}{T_s \cdot \omega \cdot (1 + \omega^2 T_0^2)^2} \cdot$$
$$\begin{pmatrix} -2\omega T_0 \cdot \left(\cos\left(\omega(t_M + t_d)\right)\sin\omega T_s + \sin\left(\omega(t_M + t_d)\right) \cdot (1 - \cos\omega T_s)\right) + \\ (1 - \omega^2 T_0^2) \cdot \left(\cos\left(\omega(t_M + t_d)\right) \cdot (1 - \cos\omega T_s) + \sin\left(\omega(t_M + t_d)\right)\sin\omega T_s\right) \end{pmatrix}$$
$$(28)$$

The argument and the phase of the $G_p(i\omega)$ is described by (29), (30)

$$\rho_p(\omega) = \left(ReG_p(\omega)^2 + ImG_p(\omega)^2\right)^{1/2} \quad (29)$$

$$\varphi_p(\omega) = \pi + \sin^{-1}\left(\frac{ImG_p(\omega)}{\rho_p(\omega)}\right) \qquad (30)$$

The PID controller transfer function follows:

$$G_c(i\omega) = k_p + i \cdot \left(k_d\omega - \frac{k_i}{\omega}\right) \qquad (31)$$

The open loop transfer function is given by the product (32):

$$G_l(i\omega) = G_p(i\omega)G_c(i\omega) \qquad (32)$$

The square of the distance of any $G_l(i\omega)$ point of the Nyquist plot to the point (-1,0) on the real axis is given by the formula:

$$f\left(k_p, k_i, k_d, \omega\right) = (ReG_l(i\omega) + 1)^2 + ImG_l(i\omega)^2 \qquad (33)$$

According to Astrom et al. [16], the robustness condition is expressed by (34):
$$f\left(k_p, k_i, k_d, \omega\right) \geq r_s \qquad (34)$$

Where $r_s=1/M_s$. The argument ω is dropped in the subsequent computations to simplify the representation.

$$\left(\frac{\rho_p}{r_s}\right)^2\left(k_p + \frac{ReG_p}{\rho_p^2}\right)^2 + \left(\frac{\rho_p}{\omega r_s}\right)^2\left(k_i - \frac{\omega ImG_p}{\rho_p^2} - \omega^2 k_d\right)^2 \geq 1 \qquad (35)$$

Then according to [16], the maximum value of k_i for constant value of k_d, occurs at the lower vertex of the ellipse (35). This point is given by the equations (36), (37):

$$k_p = -\frac{\cos\varphi_p}{\rho_p} \qquad (36)$$

$$k_i = -\frac{\omega}{\rho_p}(r_s - \sin\varphi_p) + \omega^2 k_d \qquad (37)$$

By differentiating equation (37), the maximum k_i occurs at the frequency where the derivative of k_i is equal to 0. After some computations the derivative concludes to formula (38):

$$H_{PID}(\omega) = (r_s - sin\varphi_p)\left(\frac{\rho_p'}{\rho_p} - \frac{1}{\omega}\right) + \varphi_p' cos\varphi_p$$
$$+ 2\rho_p k_d \qquad (38)$$

Where ρ_p' and φ_p' denote the derivatives of ρ_p and φ_p respectively. Equation (38) is solved iteratively by applying the bisection method and solution ω_{PID} is found. To guaranty that the solution corresponds to a maximum the condition $\frac{\partial^2 f}{\partial \omega^2} < 0$ shall be satisfied. As initial frequencies' interval for the bisection implementation the region $[\omega(\varphi=\pi/2),\omega(\varphi=\pi-sin^{-1}(r_s))$ is determined.

The procedure starts with $k_d=0$. By applying equation (24) to (38), k_p, k_i are computed. Then using a constant step, the k_d value is increased and new proportional and integral gains are calculated. The procedure continues up to the largest k_d for which the robustness condition is satisfied. Therefore the implementation of the MIGO technique provides a full group of (k_p, k_i, k_d) parameters ranging from $k_d=0$ to a maximum value fulfilling the M_s constraint as to the open loop transfer function.

3.2 Controllers' Parameterization

To investigate the impact of M_s constraint to the values of the (k_p,k_i,k_d) sets, the PID parameters are computed for the M_s range [1.3,2.5] using the average RM dynamics shown in Table 2. The results of k_p, k_i as function of M_s, k_d for the controller between %limestone and LSF are shown in Figures 5, 6. The corresponding results for the SM controller are depicted in Figures 7, 8.

Figure 5. LSF controller. K_p as function of k_d, M_s.

The following can be concluded from these figures:

- As M_s increases, the maximum k_d, $k_{d,Max}$ also enlarges. As regards the LSF parameters, for $M_s=1.3$ the maximum k_d is equal to 0.06 while for $M_s=1.6$, $k_{d,Max}$ augments to 0.1 and for $M_s=2.5$ reach the value 0.16.
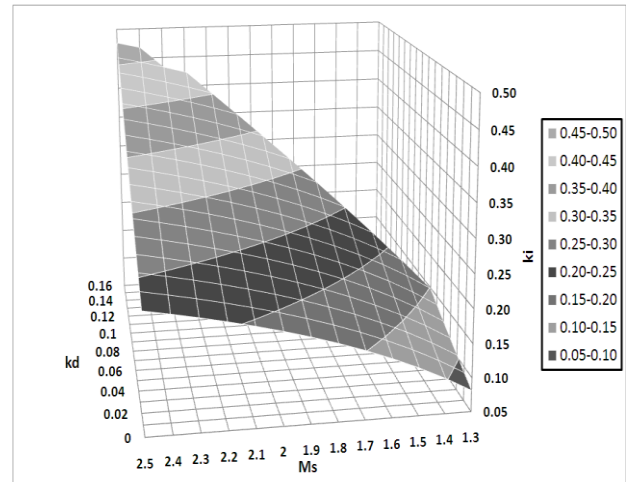

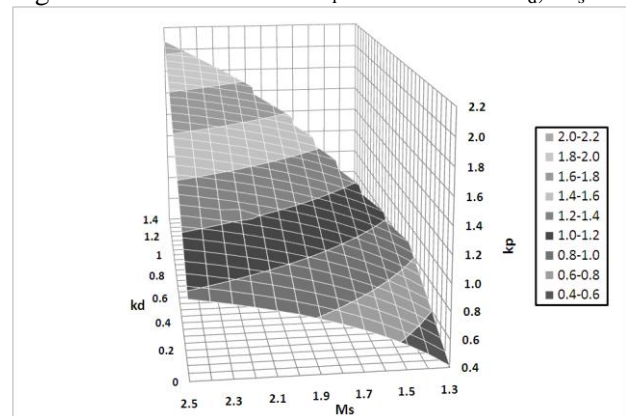Figure 6. LSF controller. K_i as function of k_d, M_s.
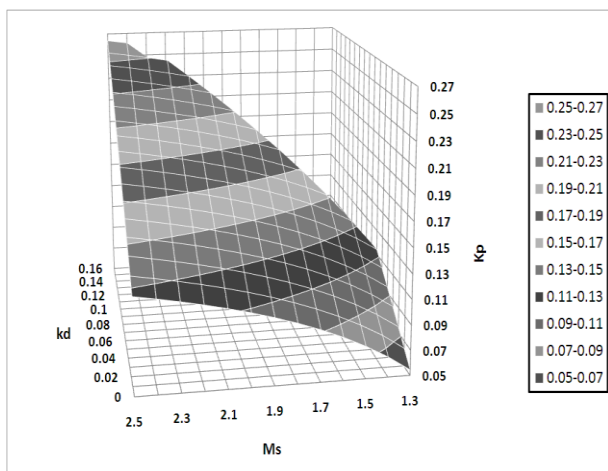

Figure 7. SM controller. K_p as function of k_d, M_s.

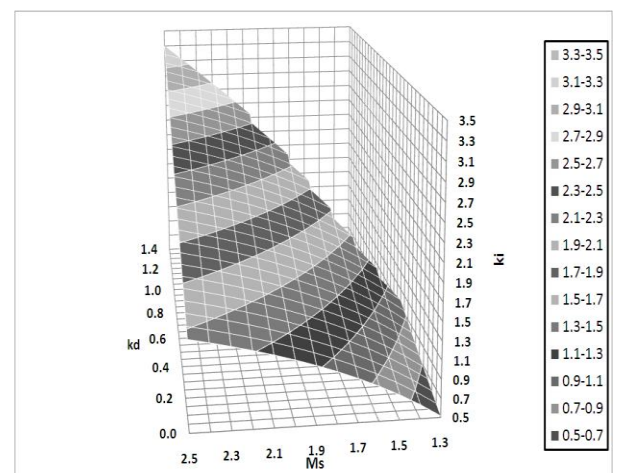Figure 8. SM controller. K_i as function of k_d, M_s.

- For any given value of M_s, as k_d increases from 0 to $k_{d,Max}$, the proportional and integral gains become around the double.

- The LSF k_p, k_i for the parameters' sets (M_s, k_d) and (M_s+0.1, k_d-0.01) are around equivalent.
- The same occurs for the sets (M_s, k_d) and (M_s+0.1, k_d-0.1), regarding the SM controller.

The above means that for the same k_p, k_i values, a lower M_s value can be obtained with an increase of the k_d value. The impact of the k_d value to the open loop Nyquist plot, for M_s=1.5 is shown in Figures 9 and 10 for the LSF and SM controllers respectively.
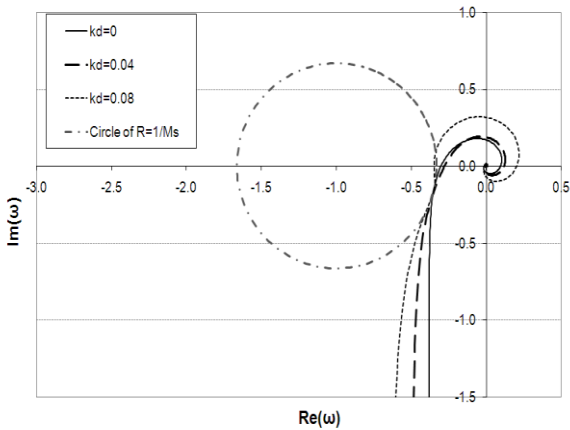

Figure 9. Niquist plots for M_s=1.5 and different k_d for the LSF controller.
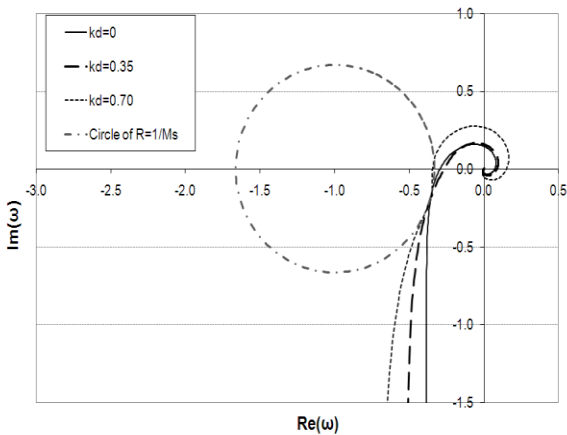
Figure 10. Niquist plots for M_s=1.5 and different k_d for the SM controller.

From these two figures it is observed that as k_d increases from 0 to the maximum value, bigger segment of the loop approaches the circle of radius $1/M_s$ by satisfying always the specified constraint.

3.3 Influence of the Model Uncertainty on the Open Loop Properties

The model parameters shown in Table 2 are the average of the values computed for each set of input and process variables. To study the effect of model parameter uncertainty on the achieved sensitivity

and gain margin of the open loop function the following procedure is implemented:

(a) A certain set of PID parameters is considered.
(b) For each set of experimental data the open loop properties are computed.
(c) The average, the standard deviation and the coefficient of variation, %CV, of each property are found.
(d) The above procedure is applied for all PID sets for M_s range [1.3, 1.9] and k_d range [0, $k_{d,Max}$]

The M_s distribution for M_s design value equal to 1.5 and k_d = 0, 0.04, 0.08 are depicted in Figure 11 for the LSF controller. Up to k_d=0.04 the distribution appears steep enough. For k_d=0.08 the distribution variance increases drastically and a significant portion of the experimental sets - ~20% - presents $M_s \geq 2.0$. Therefore for the 20% of the actual data the maximum k_d controller becomes less robust.
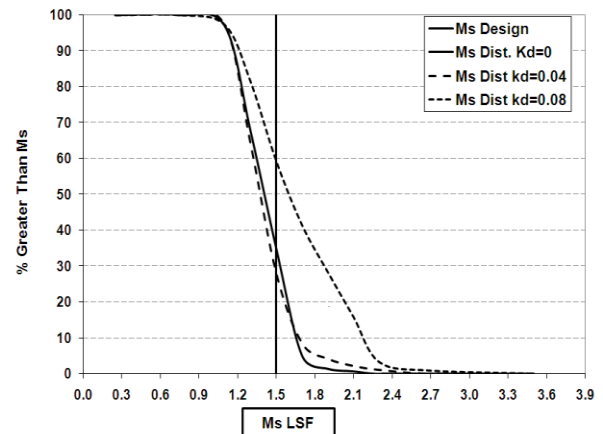

Figure 11. M_s distribution for $M_{s,Design}$=1.5. LSF controller.

The average actual M_s and g_m over all the data sets as function of the design M_s and k_d are shown in Figures 12, 13 for the LSF controller.
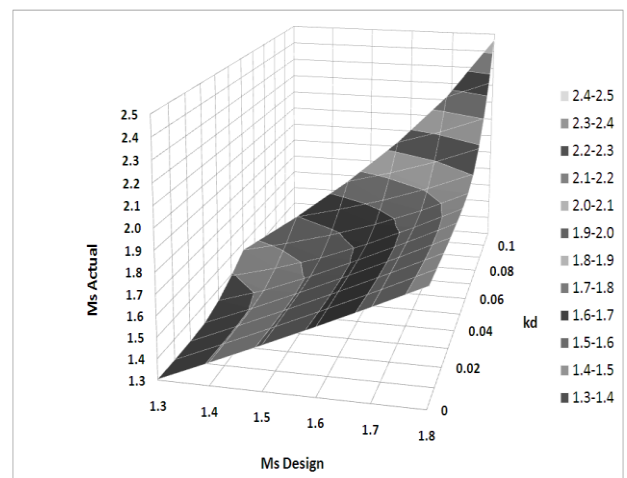

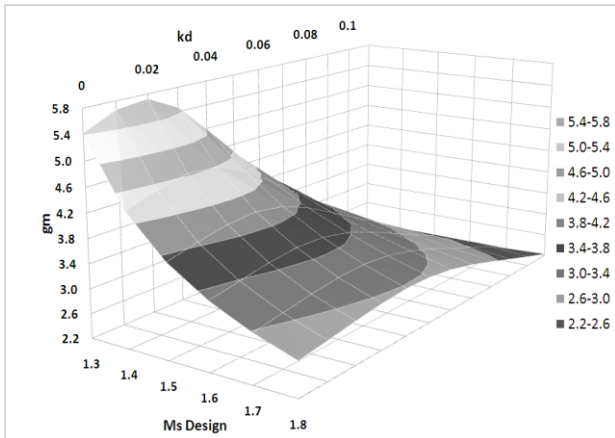Figure 12. Average M_s as function $M_{s,Design}$ and k_d. LSF controller.

Figure 13. Average g_m as function $M_{s,Design}$ and k_d. LSF controller.

The investigation of these figures leads to the following remarks:

(a) For a certain value of the design maximum sensitivity, $M_{s,D}$, the realized average M_s remains close to $M_{s,D}$ for $0 \leq k_d \leq k_d^*$, where k_d^* is located around to the middle of the range $[0,k_{d,Max}]$. Then as k_d augments, average M_s rises significantly. To elucidate further this trend the $M_s/M_{s,D}$ ratio is plotted as function of $M_{s,D}$ and k_d. The results are depicted in Figure 14.

(b) As k_d increases, the gain margin passes from a maximum, placed near to the centre of $[0,k_{d,Max}]$.

(c) The previous two remarks mean that for a specified $M_{s,D}$ value a good compromise of performance and robustness can be achieved by selecting a set of PID parameters with k_d located near to the midpoint of the permissible range $[0,k_{d,Max}]$
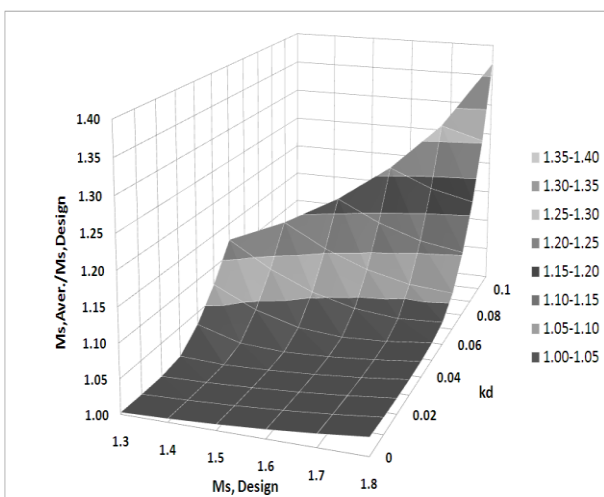

Figure 14. $M_s/M_{s,D}$ as function $M_{s,D}$ and k_d. LSF controller.

The coefficients of variation, %CV, of M_s and g_m over all the data sets are demonstrated in Figures 15,

16. For M_s values belonging to the range [1.3, 1.7] and k_d from 0 up to the middle of the maximum, the %CV is rising slowly. Then the rate of increase is higher. For M_s=1.8, the %CV increases linearly as k_d varies from 0 to $k_{d,Max}$. The above verifies that for k_d higher than the midpoint of the range, the controller robustness seems to be deteriorated. Nevertheless if an $M_{s,Design}$ reasonably low is selected, the actual M_s is not so high. Apparently a simulation of the real process is expected to lead to more rigorous optimization of the PID coefficients. The %CV of g_m remains in the level of 37% to 43% for all the M_s and k_d ranges examined.
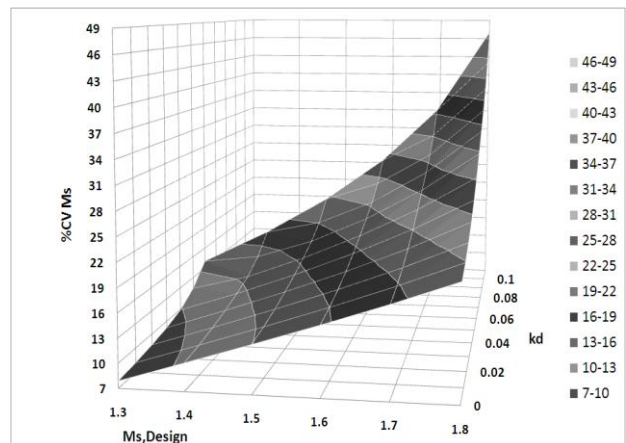

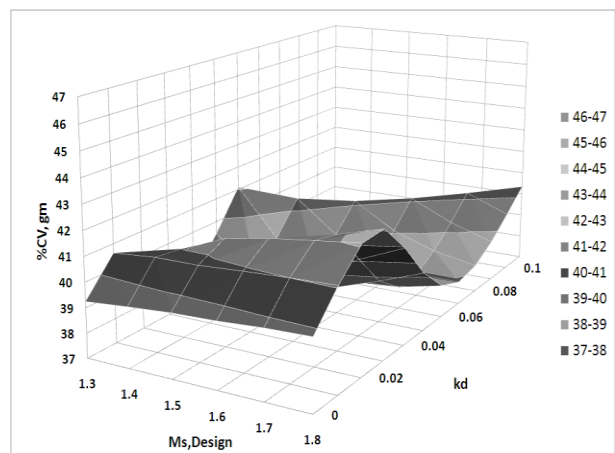Figure 15. %CV of M_s as function $M_{s,Design}$ and k_d. LSF controller.

Figure 16. %CV of g_m as function $M_{s,Design}$ and k_d. LSF controller.

As regards the SM controller, the functions between the average values of M_s and g_m and $M_{s,D}$, k_d are shown in Figures 17,18. The $M_s/M_{s,D}$ ratio respective function appears in Figure 19. The interval [1.3, 1.6] is chosen as M_s range. The k_d values are restricted up to $k_{d,Max}$=0.75. For $M_s > 1.6$ and $k_d > 0.75$, there are data sets where the closed loop becomes unstable. The conclusions drawn for the PID parameters of the LSF controller are also

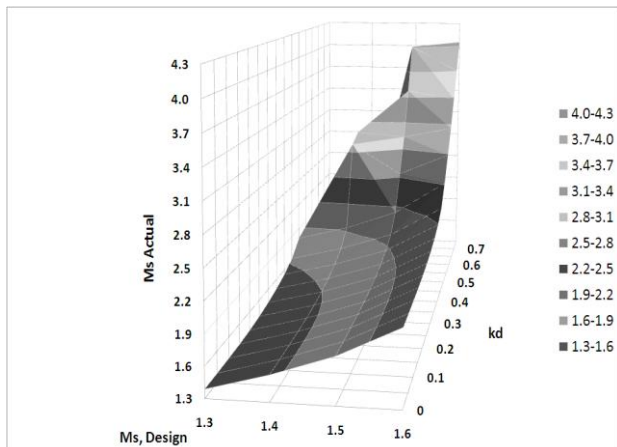valid for the corresponding parameters of the SM controller.

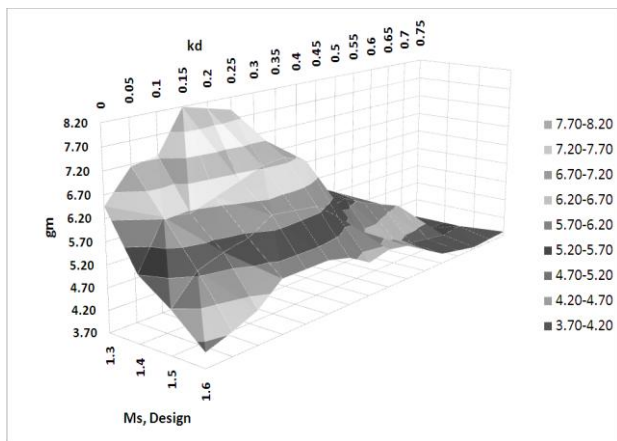Figure 17. Average M_s as function $M_{s,D}$ and k_d. SM controller.

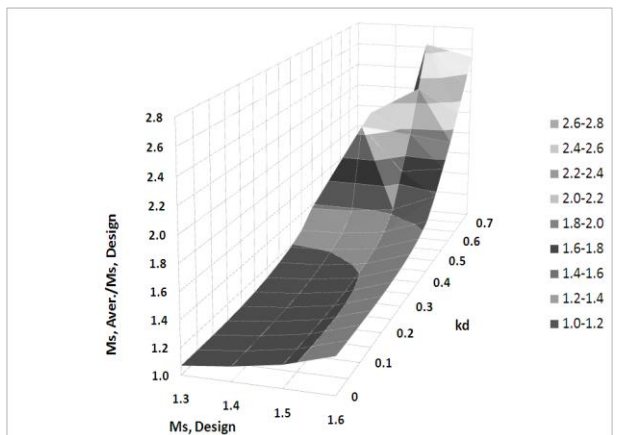Figure 18. Average g_m as function $M_{s,D}$ and k_d. SM controller.

Figure 19. $M_s/M_{s,D}$ as function $M_{s,D}$ and k_d. SM controller.

4   Application of the Controller

The results of application of the controller for a 17 months period for the regulation of the raw meal in Halyps plant are demonstrated and analyzed. Before

the implementation of the current version of the PID controller the LSF and SM modules in the RM outlet were regulated using a PI controller presented in [19]. The PID is initially parameterized off line with the MIGO method using one year actual plant data. Then using the last months' data the parameters are checked as regards the sensitivity of the open loop and retuned if necessary. As design parameters, M_s=1.5 and k_d located in the middle of the permissible range are chosen. The standard deviation results of the modules are compared with the ones of the long term implementation of the PI controller which has been running continuously for more than ten years providing a remarkable improvement of the raw meal quality, compared with the manual regulation.

Results are also presented of PID controllers' applications tuned with the MIGO technique and putted into operation in other plants. These results are compared with the ones of operation before the PID installation.

4.1 Standard Deviation of LSF and SM in the Mill Outlet and Kiln Feed

As evaluation indicator of quality performance the standard deviation of the variable under examination is considered. This standard deviation is calculated over all the available results for a specified period. The monthly standard deviation of LSF in the RM outlet is shown in Figure 20. The population of the results is composed from all the hourly analysis of samples taken in the RM exit, before the homogenization silo. These results indicate that there is a noticeable reduction of the LSF variance after the new PID operation. The range also of the monthly standard deviation is narrower than the one corresponding to PI controller. The above can be thought as a consequence of the sensitivity condition satisfied implicitly.
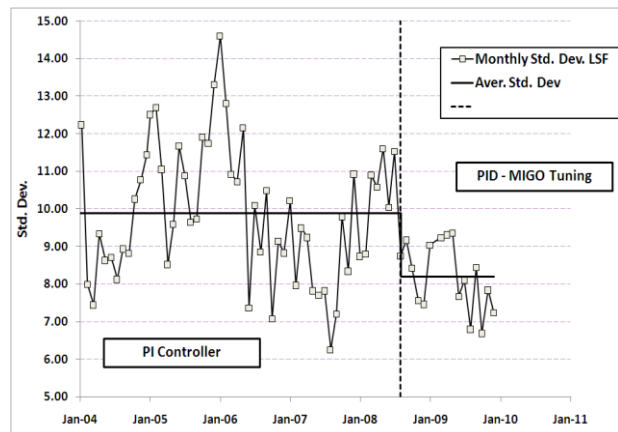

Figure 20. Monthly LSF standard deviation in the RM exit.

The LSF monthly standard deviation of the kiln feed spot samples are depicted in Figure 21. The sampling period for the given sampling system is four hours and the raw meal is sampled in the stock silo outlet before to be fed to the kiln.
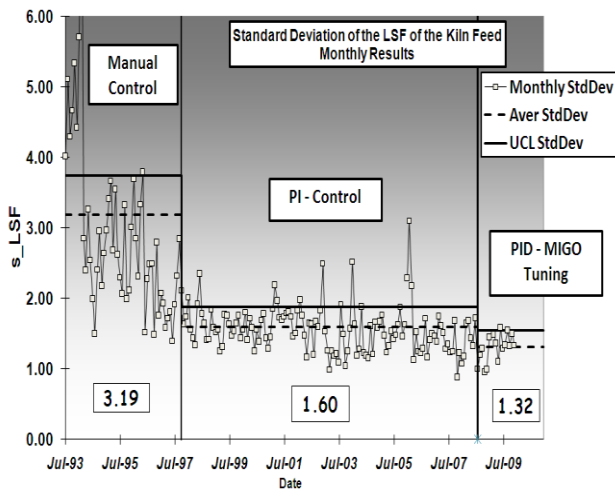

Figure 21. Monthly LSF standard deviation in the kiln feed.

Three periods are indicated in Figure 21:
- August 2008 – December 2009 of PID operation.
- October 1997-July 2008, the period of the PI continuous and long term implementation
- July 1993 – September 1997 where the raw meal quality was regulated by applying written instructions and the operator's experience, manually.

Not only the average standard deviation appears in the figure, but also its upper control limit (UCL) according to ISO 8258:1991. The formulae to compute the UCL for this specific application are described in [19].   As it is also analytically illustrated in [19], the PI controller tuned with a specific technique, provided a huge amendment of the raw meal homogeneity. Sensitivity criteria were taken into account to this method, but an embedded criterion of robustness was not involved. The above fact could be the reason that 15 out of 130 monthly deviations - 11.5% - are higher of the UCL, which is equal to 1.87. On the opposite after the implementation of the MIGO methodology, where the sensitivity robustness condition is implied, not only the average deviation is significantly lower but only 1 out of 16 -or 6.3% - is higher that the UCL that is only 1.54, minor than the average deviation during the PI implementation. Therefore the tuning by the MIGO technique appears to be very effective, under normal operating conditions.

The same results for the SM module are presented in Figures 22, 23.
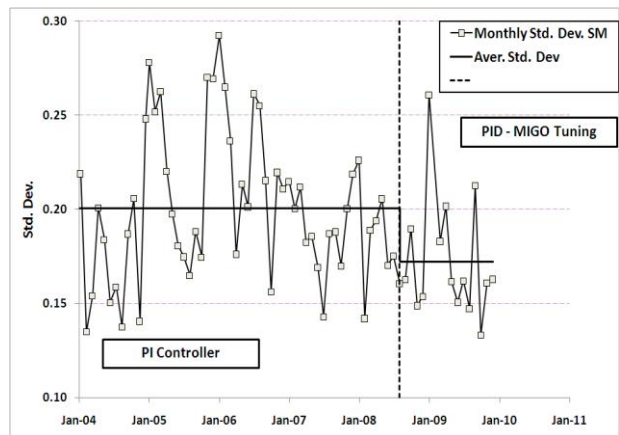

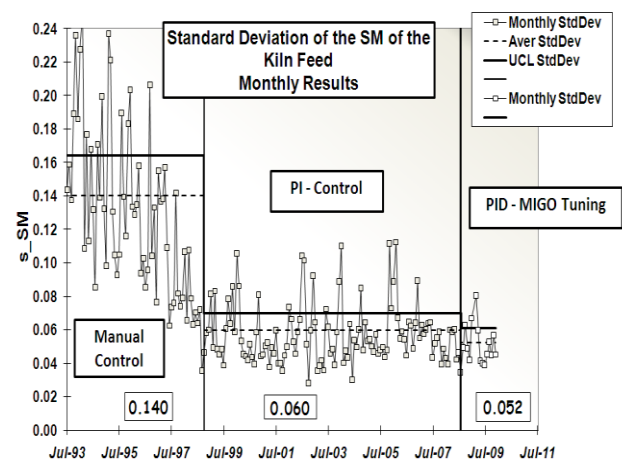Figure 22. Monthly SM standard deviation in the RM exit.

Figure 23. Monthly SM standard deviation in the kiln feed.

The same conclusions drawn from the Figures shown the LSF variance are also valid for the SM one. During the PI operation 20 out of 118 points – 16.9% - are higher than the UCL. On the other hand the PID installation led to a decrease of the average deviation and of the UCL as well, which is positioned very near to the average of the PI operation.

Table 3. Annual quality indicators

Year	s RM LSF	s KF LSF	%Num. of Cuts	s RM SM	s KF SM	%Num. of Cuts
2005	11.2	1.58	36.3	0.23	0.062	28.4
2006	10.5	1.67	36.1	0.23	0.072	25.4
2007	8.8	1.46	37.3	0.19	0.057	25.8
1-7 2008	10.6	1.56	37.9	0.19	0.053	29.3
8-12 2008	8.3	1.11	39.3	0.16	0.050	29.5
2009	8.1	1.44	38.7	0.18	0.052	30.6

The quality indicators in annual basis are also presented in Table 3 from 2005 to 2009. The percentage of times the module values pass from the

target to the total samples' population - the %Number of Cuts – is also calculated. The first four rows correspond to PI operation while the last two ones to PID functioning. During the new controller implementation not only a lower deviation in RM outlet is achieved, but also an increase of the %Number of cuts. Especially the second result produces more and thinner layers of raw meal into the homo and stock silos contributing to a better mixing and the respective reduction of variance in the raw meal fed to the kiln.

4.2 Other Implementations of the PID Controller Tuned with the MIGO Method

The method applied to tune the PID driving the raw meal quality control of Halyps and the software developed, were also putted in operation to other plants of Italcementi Group in Egypt, regulating a severe number of raw mills. Each kiln of these plants is fed with raw meal produced from one or two RM. Before the installation of the controllers, the quality regulation was performed in manual mode. Results of LSF monthly standard deviation of the raw meal in the kiln feed are demonstrated in Figures 24 to 27.
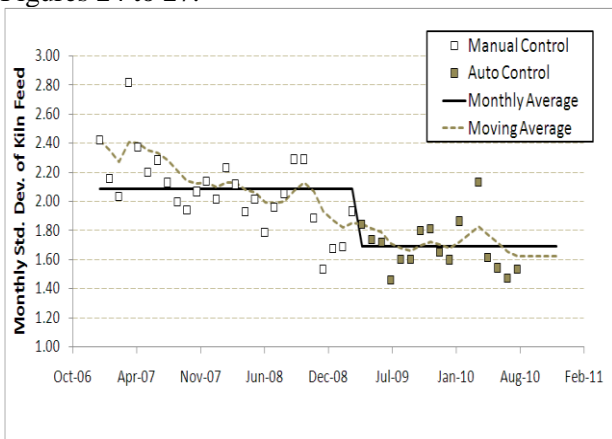

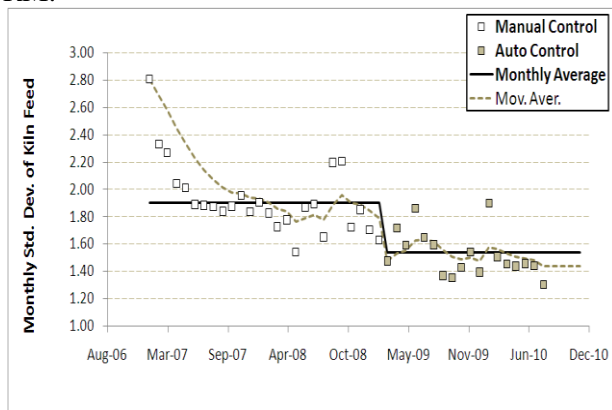Figure 24. Plant 1. Kiln 1 raw meal feed from one RM.

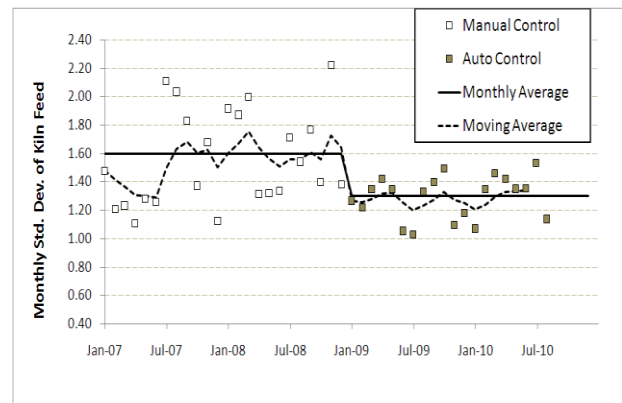Figure 25. Plant 1. Kiln 2 raw meal feed from one RM.

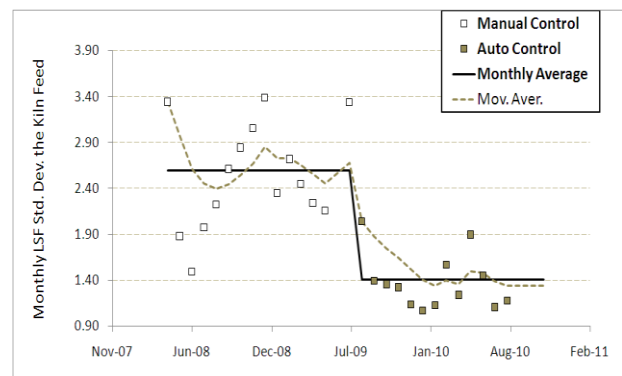Figure 26. Plant 2. Kiln 1 raw meal feed from one RM.

Figure 27. Plant 3. Kiln 1 raw meal feed from two RM.

In Table 4 the average standard deviations are summarized, before and after the installation of the PID controller software, s_b and s_a respectively.

Table 4. Kiln feed standard deviation before and after the PID installation.

Plant, kiln	s_b	s_a	$s_b - s_a$
Plant 1, kiln 1	2.09	1.69	0.40
Plant 1, kiln 2	1.90	1.54	0.36
Plant 2, kiln 1	1.60	1.30	0.30
Plant 3, kiln 1	2.60	1.41	1.19

The operation of the PID controllers parameterized with the MIGO technique provides a step decrease of the raw meal standard deviation resulting in a distinguishable amendment of the product quality delivering improved economic performance in cement production [36].

5   Conclusions

Based on a dynamical model of the raw materials mixing in closed circuit ball mill, efficient efforts were accomplished to parameterize a PID controller regulating a high importance process from the quality and production point of view. The settings of the limestone and additive weight feeders consist of

the set of the two control variables. As process variables the Lime Saturation Factor and the Silica Modulus are chosen. For the TITO process under investigation and the current raw materials' quality the two loops interaction is extremely week at low frequencies according to the Relative Gain Array results.

The two controllers' tuning is realized by applying the M-constrained integral gain optimization technique to the specific conditions of raw meal production and quality control. By utilizing seven months industrial raw data, the dynamical model parameters are determined. Afterwards sets (k_p, k_i, k_d) are computed for maximum sensitivity $1.3 \leq M_s \leq 2.5$. M_s constitutes the robustness criterion and it can be thought as the principal design parameter. For a specified M_s, a family of (k_p, k_i, k_d) sets is determined starting from $k_d=0$ up a maximum value $k_{d,Max}$, satisfying the robustness constraint. Using the industrial data sets, for each PID parameter set the actual M_s and gain margin as found. In the current level of development of the research, among these PID sets, it is selected the one having design $M_s=1.5$, actual M_s not differing significantly from the designed one and the higher possible k_d. This set is found near to the middle of the [0, $k_{d,Max}$] interval.

The described methodology of tuning is implemented in the raw meal grinding system of Halyps cement plant, where an efficient PI controller was operating for more than ten years deriving a huge amendment of the raw meal quality. The technique of this controller tuning is described in [19]. The implementation of the PID version analyzed to this study resulted in a noticeable increase of homogeneity of the raw meal fed to the kiln. The same technique of tuning was also applied to other raw meal grinding systems, previously operating in manual mode as concerns the chemical modules regulation. The PID implementation software was built, installed and operated. According to the results presented after a sufficient period of operation, the raw meal standard deviation in the kiln feed approached satisfactorily the levels achieved in Halyps installations. Therefore the current implementation of the M-constrained integral gain optimization contributed remarkably to the effectiveness of the raw meal quality control in a noticeable number of industrial installations.

A further and deeper development of the robust and effective control of the raw meal quality could investigate the following issues:

- With the acceptance of the M_s robustness constraint as design criterion, to simulate the raw mill, homo and stock silos operation, specific for each plant, to find the optimum PID set.
- To examine whether the chemical modules in the homo or stock silos, predicted with the model, can be fed back as an outer loop to provide set point to the raw mill controller, resulting in a cascade control.
- By utilizing model predictive control (MPC) techniques and respecting the robustness constraints, to predict the chemical modules in the RM or the silos outlet supposing constant raw materials and to tune the controller accordingly. Extensive simulations are always necessary before to apply the findings in actual raw meal systems.

References:
[1] Lee, F.M., The Chemistry of Cement and Concrete,*3rd ed. Chemical Publishing Company, Inc.*, New York, 1971, pp. 164-165, 171-174, 384-387.
[2] Bond, J.E., Coursaux, R., Worthington, R.L., Blending systems and control technologies for cement raw materials, *IEEE Industry Applications Magazine*, Vol. 6, 2000, pp.49-59.
[3] Ozsoy, C. Kural, A. Baykara, C. , Modeling of the raw mixing process in cement industry, *Proceedings of 8th IEEE International Conference on Emerging Technologies and Factory Automation,* 2001*,* Vol. 1, pp. 475-482.
[4] Kizilaslan, K., Ertugrul, S., Kural, A., Ozsoy, C., A comparative study on modeling of a raw material blending process in cement industry using conventional and intelligent techniques, *Proceedings of IEEE Conference on Control Applications*, Vol. 1, 2003,pp. 736-741
[5] Kural, A., Özsoy, C., Identification and control of the raw material blending process in cement industry, *International Journal of Adaptive Control and Signal Processing,* Vol. 18, 2004, pp. 427-442.
[6] Tsamatsoulis, D., Modeling of Raw Material Mixing Process in Raw Meal Grinding Installations, *WSEAS Transactions on Systems and Control*, Vol. 5, 2010, pp. 779-791.
[7] Jing, J., Yingying, Y., Yanxian, F., Optimal Sliding-mode Control Scheme for the Position Tracking Servo System, *WSEAS Transactions on Systems*, Vol. 7, 2008, pp. 435-444.
[8] Bagdasaryan, A., System Approach to Synthesis, Modeling and Control of Complex Dynamical Systems, *WSEAS Transactions on Systems and Control*, Vol. 4, 2009, pp. 77-87.
[9] Emami, T., Watkins, J.M., Robust Performance Characterization of PID Controllers in the

Frequency Domain, *WSEAS Transactions on Systems and Control*, Vol. 4, 2009, pp. 232-242.

[10] Tsamatsoulis, D., Dynamic Behavior of Closed Grinding Systems and Effective PID Parameterization, *WSEAS Transactions on Systems and Control*, Vol. 4, 2009, pp. 581-602.

[11] Keviczky, L., Hetthéssy, J., Hilger, M. and Kolostori, J., Self-tuning adaptive control of cement raw material blending, *Automatica*, Vol. 14, 1978, pp.525-532.

[12] Banyasz, C. Keviczky, L. Vajk, I. A novel adaptive control system for raw material blending process, *Control Systems Magazine*, Vol. 23, 2003, pp. 87-96.

[13] Duan, X., Yang, C., Li, H., Gui, W., Deng, H., Hybrid expert system for raw materials blending, *Control Engineering Practice,* Vol. 16, 2008, pp. 1364-1371.

[14] Bavdaz, G., Kocijan, J., Fuzzy controller for cement raw material blending, *Transactions of the Institute of Measurement and Control*, Vol. 29, 2007, pp. 17-34.

[15] Zhugang Yuan, Zhiyuan Liu, Run Pei, Fuzzy control of cement raw meal production, *Proceedings of IEEE International Conference on Automation and Logistics*, 2008. Pp. 1619-1624.

[16] Astrom, K., Hagglund, T., Advanced PID Control, *Research Triangle Park: Instrumentation, Systems and Automatic Society,* 2006.

[17] Ender, D., Process Control Performance: Not as good as you think, *Control Engineering*, Vol. 40, 1993, pp.180-190

[18] Gao, Z., Scaling and bandwidth - parameterization based controller tuning, *Proceedings of the American Control Conference*, Vol. 6, 2003, pp. 4989-4996.

[19] Tsamatsoulis, D., Development and Application of a Cement Raw Meal Controller, *Ind. Eng. Chem. Res.,* Vol. 44, 2005, pp. 7164-7174.

[20] Astrom. K.J., Model Uncertainty and Robust Control, *Lecture Notes on Iterative Identification and Control Design,* Lund University, 2000, pp. 63–100.

[21] Zolotas, A.C., Halikias, G.D., Optimal Design of PID Controllers Using the QFT Method, IEE Proc. – Control Theory Appl., Vol. 146, 1999, pp. 585-590

[22] Gorinevsky, D., Loop-shaping for Iterative Control of Batch Processes, *IEEE Control Systems Magazine*, Vol. 22, 2002, pp. 55—65.

[23] Yaniv, O., Nagurka, M. Automatic Loop Shaping of Structured Controllers Satisfying QFT Performance, *Transactions of the ASME*, Vol. 125, 2005, pp. 472-477.

[24] McFarlane, D., Glover, K., A loop shaping design procedure using H_∞ synthesis, *IEEE Transactions on Automatic Control*, Vol. 37, 1992, pp. 759–769.

[25] Isidori, A., Astolfi, A., Disturbance attenuation and H_∞-Control via measurement feedback in non-linear systems, *IEEE Transactions on Automatic Control*, Vol. 37, 1992, pp.1283-1293.

[26] Lu, G., Ho, D., On robust H_∞ control for non-linear uncertain systems, *Communications in Information and Systems*, Vol. 2, 2002, pp.255-264.

[27] Shen, J., H_∞ control and sliding mode control of magnetic levitation system, *Asian Journal of Control*, Vol. 4, 2002, pp. 333-340.

[28] Kim, J.H., Oh, D.C., Robust and Non-fragile H_∞ Control for Descriptor Systems with Parameter Uncertainties and Time Delay, *International Journal of Control*, Automation, and Systems, Vol. 5, 2007, pp. 8-14.

[29] Fakharian, A., Jamshidi, F., Taghi, M., Beheshti, H., Ardestani, M., Switching H_2 /H_∞ Control of Singular Perturbation Systems.

[30] Sourkounis, C., Active Dynamic damping of torsional vibrations by H_∞ - Control, *Proceedings of 12th International Conference on Optimization of Electrical and Electronic Equipment*, Brasov, 2010, pp. IACM 4.1.08

[31] Astrom, K.J., Panagopoulos, H., Hagglund, T., Design of PI controllers based on non-convex optimization, *Automatica*, Vol. 34, 1998, pp. 585–601.

[32] Hagglund, T., Astrom, K.J., Revisiting the Ziegler–Nichols tuning rules for PI control, Asian Journal of Control, Vol. 4, 2002, pp. 364–380.

[33] Panagopoulos, H. Astrom, K.J., Hagglund, T., Design of PID controllers based on constrained optimization, *IEE Proceedings-Control Theory and Applications*, Vol. 149, 2002, pp. 32–40.

[34] Astrom, K.J., Hagglund, T., Revisiting the Ziegler–Nichols step response method for PID control, *Journal of Process Control*, Vol. 14, 2004, pp. 635–650.

[35] Bristol, E., On a new measure of interactions for multivariable process control, IEEE Transactions on Automatic Control, Vol. 11, 1966, pp. 133-134.

[36] Gordon, L., Advanced raw mill control delivers improved economic performance in cement production, *IEEE Cement Industry Technical Conference*, 2004, pp. 263-272.